6-1-2010

A Comparison of Methods for Determining Significant Wave Heights-Applied to a 3-m Discus Buoy during Hurricane Katrina

Leslie C. Bender III
Texas A&M University, les@gerg.tamu.edu

Norman Guinasso
Texas A&M University, guinasso@tamu.edu

John N. Walpert
Texas A&M University, walpert@gerg.tamu.edu

Stephan D. Howden
University of Southern Mississippi, stephan.howden@usm.edu

A Comparison of Methods for Determining Significant Wave Heights—Applied to a 3-m Discus Buoy during Hurricane Katrina

L. C. BENDER III, N. L. GUINASSO JR., AND J. N. WALPERT

Geochemical and Environmental Research Group, Texas A&M University, College Station, Texas

S. D. HOWDEN

Department of Marine Science, University of Southern Mississippi, Stennis Space Center, Mississippi

ABSTRACT

In August 2005, the eye of Hurricane Katrina passed 90 km to the west of a 3-m discus buoy deployed in the Mississippi Sound and operated by the Central Gulf of Mexico Ocean Observing System (CenGOOS). The buoy motions were measured with a strapped-down, 6 degrees of freedom accelerometer, a three-axis magnetometer, and from the displacement of a GPS antenna measured by postprocessed-kinematic GPS. Recognizing that an accelerometer experiences a large offset due to gravity, the authors investigated four different means of computing wave heights. In the most widely used method for a buoy with a strapped-down, 1D accelerometer, wave heights are overestimated by 26% on average and up to 56% during the peak of the hurricane. In the second method, the component of gravity is removed from the deck relative z-axis accelerations, requiring pitch and roll information. This is most similar to the motion of the GPS antenna and reduces the overestimation to only 5% on average. In the third method, the orientation data are used to obtain a very accurate estimate of the vertical acceleration, reducing the overestimation of wave heights to 1%. The fourth method computes an estimate of the true earth-referenced vertical accelerations using the accelerations from all three axes but not the pitch and roll information. It underestimates the wave heights by 2.5%. The fifth method uses the acceleration from all three axes and the pitch and roll information to obtain the earth-referenced vertical acceleration of the buoy, the most accurate measure of the true wave vertical acceleration. The primary conclusion of this work is that the measured deck relative accelerations from a strapped-down, 1D accelerometer must be tilt corrected in environments of high wave heights.

1. Introduction

Determining wave heights from an accelerometer mounted in a discus buoy is not necessarily straightforward. This is simply because an accelerometer measures a gravity offset along with the acceleration of the buoy and any orientation of the accelerometer that is not vertical places a component of gravity in each of the instruments' three orthogonal axes. Failure to properly account for this offset can lead to errors in the significant wave heights, particularly when the buoy is heeled over for long periods of time. In this paper, we discuss the potential difficulties that one must recognize, the

consequences of not accounting for these nuances, and four methods for removing the gravity offset from the accelerometer data. The primary means of presenting this information is through the accelerometer data obtained from a 3-m discus buoy that experienced Hurricane Katrina.

The buoy was deployed on 18 December 2004 for the University of Southern Mississippi (USM) in the Mississippi Bight on the 19-m isobath (see Fig. 1) and was recovered on 20 September 2005, following the passage of Hurricane Katrina. The buoy was funded in part to evaluate the feasibility of extending the range that postprocessed-kinematic GPS and by extension real-time kinematic (RTK) positioning could be used in the marine environment (Howden et al. 2004). The buoy was outfitted with three instruments for measuring wave-induced motion, a Novatel OEM4-g2 GPS receiver, a Crossbow IMU400CC accelerometer, and a Honeywell

Corresponding author address: Leslie C. Bender III, Geochemical and Environmental Research Group, Texas A&M University, 833 Graham Rd., College Station, TX 77845.
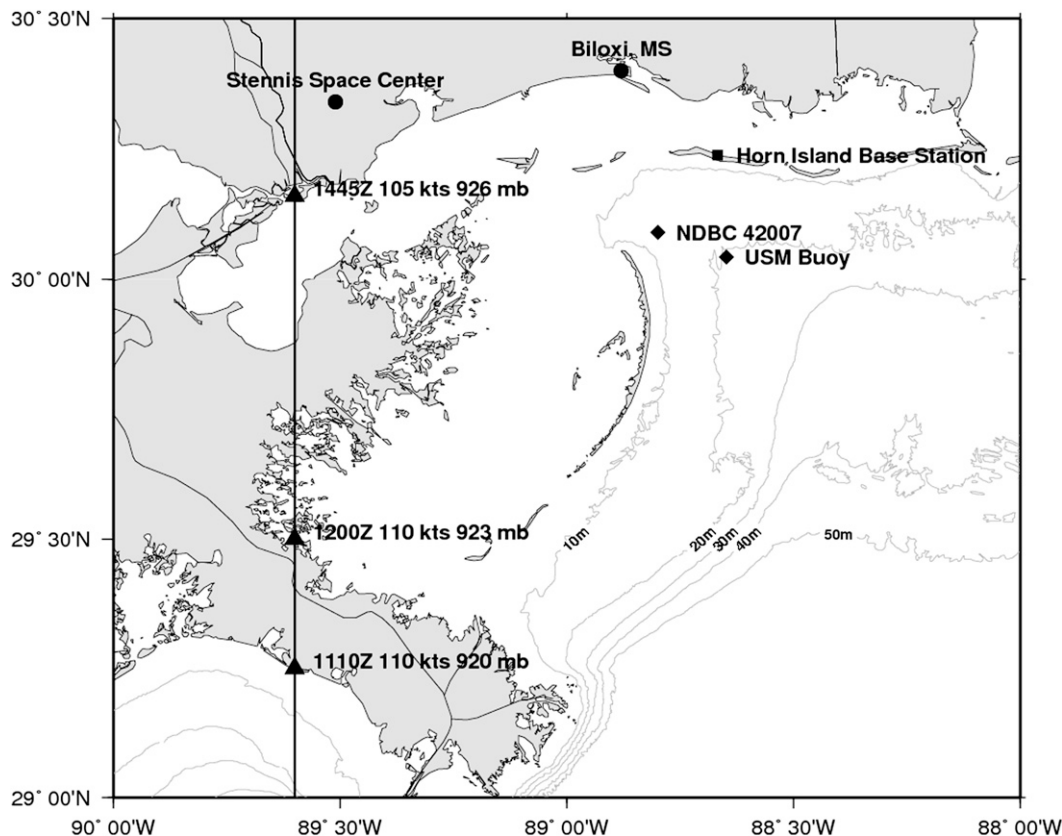E-mail: les@gerg.tamu.edu

FIG. 1. Location of the USM buoy, the NDBC buoy, and the GPS base station in the Mississippi Sound and the path of Hurricane Katrina on 29 Aug 2005.

HMR compass. In addition, the buoy had a suite of instruments for monitoring local meteorological and oceanographic conditions. The system design, electronics, and sensor integration were done independently by the Geochemical and Environmental Research Group (GERG) at Texas A&M University. GERG has operated and maintained the Texas Automated Buoy System (TABS) on behalf of the Texas General Land Office since 1995 (Bender et al. 2007). Only the mooring system was designed and built by the National Oceanic and Atmospheric Administration's (NOAA) National Data Buoy Center (NDBC) at Stennis Space Center in Stennis, Mississippi.

On 29 August 2005 at approximately 1400 UTC, the eye of Hurricane Katrina passed 90 km to the west of the buoy's location (Fig. 1). The buoy operated continuously through the storm and provided real-time data. Meteorological data from the buoy during this event has been described by Howden et al. (2008). The buoy, mooring, and 3850 kg in air concrete anchor were moved slightly to the northeast during the final approach of Katrina, but following the hurricane's landfall, and from what would appear to be a direct result of the storm

surge relaxation, the buoy was relocated to the southeast during the 8 h from 1500 to 2300 UTC (Fig. 2). The buoy experienced sustained tilts, or heels, of 15°–18° during Katrina that were directly recorded by the compass/magnetometer and indirectly measured by the pitch and roll rate sensors of the accelerometer. The GPS receiver on the buoy operated continuously through the storm, but the base station at nearby Horn Island was disabled by the storm at 0727 UTC 29 August. The ability to obtain precise vertical positions of the buoy using PPK positioning was lost at this point. All sensors' raw data were saved onboard the buoy's computer and retrieved when the buoy was recovered on 20 September 2005.

The GPS and accelerometer motion sensor data from the USM buoy provided two independent data sources that are used to determine significant wave heights. This paper describes the instrument setup of the buoy, the data obtained, and the methods used to process the accelerometer and GPS data into significant wave heights. We focus on the wave record during Hurricane Katrina and use this data to compare four methods of calculating wave heights from a strapped-down accelerometer.
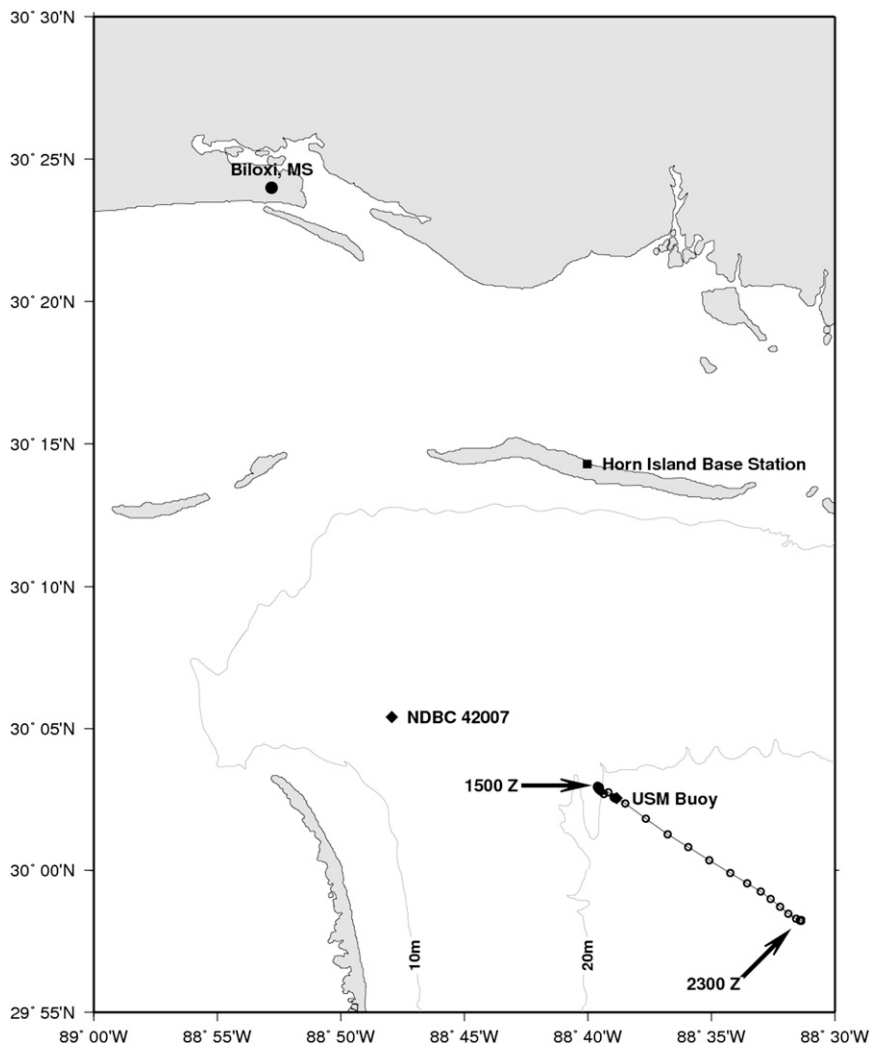
FIG. 2. Location of the USM buoy while it was dragged out to sea during the storm surge relaxation following Hurricane Katrina at 1500–2300 UTC 29 Aug 2005. The buoy came to rest at the location marked 2300 Z.

2. Instrumentation

The Crossbow IMU400CC series accelerometer measures the linear acceleration along three orthogonal axes and the rotation rates around the same three orthogonal axes. The unit was mounted (strapped-down) inside the system controller housing within the instrument well of the buoy. The sensor was installed along the centerline of the buoy at approximately the waterline and aligned so that its positive z axis was oriented down and normal to the deck of the buoy (also known as mast parallel, the standard orientation for this unit so that it measures a $+1$ g when at rest), while the positive x axis pointed to the buoy's stern and the positive y axis to the buoy's port. The accelerometer was cycled on for the first 20 min of each hour and then cycled off for the remaining 40 min.

The 4-Hz data available for this study covered the first 20 min of every hour from 5 August to 20 September 2005.

The Honeywell HMR 3300 digital compass is a solid-state three-axis magnetometer-based compass that uses an internal two-axis accelerometer for enhanced operation. This electronically gimbaled compass gives accurate headings even when the compass is tilted at 60°; though this never occurred even during the height of Katrina. The 4-Hz data available for this study covered the period from 18 April to 20 September 2005.

The Novatel OEM4-G2 GPS is a parallel 24-channel, dual-frequency, survey-grade GPS receiver. A time series of three-dimensional positions of the GPS antenna on the buoy is determined using PPK techniques on 1-Hz dual-frequency data logged on both the buoy and a GPS

receiver that was located on Horn Island, about 20 km to the north of the buoy (Howden et al. 2004; Dodd et al. 2006). Although the GPS receiver on the buoy logged data throughout the storm, the PPK positions could only be processed through 0700 UTC on 29 August 2005, after which the battery bank for the Horn Island base station was washed into the Mississippi Sound.

3. Processing

One-dimensional displacement spectra were calculated from the accelerometer data and the GPS displacement data. The development of the spectra is discussed in this section.

a. Accelerometer

An accelerometer is a device that senses the inertial reaction of a proof mass for the purposes of measuring linear or angular acceleration. In its basic form, all accelerometers consist of a spring and mass arrangement in which displacement of the mass from its rest position is proportional to the total nongravitational acceleration experienced along the instrument's axes. By definition nongravitational acceleration is produced by simple forces of motion other than gravity or inertial forces. This means that an accelerometer in free fall will not register any gravitational acceleration, but when the unit is held stationary, the accelerometer will experience an offset due to local gravity. Somewhat counterintuitively, this means that the accelerometer will indicate +1 g along the vertical axis *away* from the earth. For an earthbound accelerometer, the attractive force of gravity acting on the proof mass is treated as an applied upward acceleration of +1 g. This is the accepted standard definition promulgated by Institute of Electrical and Electronic Engineers (1994).

The Crossbow IMU400 does not follow the IEEE definition for gravity, though Crossbow's newer instruments do. The IMU400 orients z positive down in a right-handed coordinate system and defines gravitational acceleration as +1 g directed downward. Given proper care of the signs, however, this does not affect the final measurements. The IMU400 reports accelerations in g's so that the three sensors measure the following:

$$X_S = \frac{-a_x + g_x}{g}$$
$$Y_S = \frac{-a_y + g_y}{g}$$
$$Z_S = \frac{-a_z + g_z}{g}, \qquad (1)$$

where a_x, a_y, and a_z are the nongravitational buoy accelerations; g_x, g_y, and g_z are the components of the plumb bob gravity along the x, y, and z axes; g is the gravitational acceleration; and X_S, Y_S, and Z_S are what the accelerometer records.

Removing the component of gravity from the X_S, Y_S, and Z_S data recorded by each the accelerometer requires either direct information about the orientation of the sensor relative to the earth coordinate frame or an assumption about the buoy tilt. The exact method of correcting for the buoy's tilt is to mathematically rotate the three axes' accelerations from the sensor frame to the earth coordinate frame. Because 3D rotations do not commute, we rely on direction cosines to obtain the earth referenced z acceleration, or Z_E in this case,

$$\begin{bmatrix} X_E \\ Y_E \\ Z_E \end{bmatrix} = \begin{bmatrix} a_1 & b_1 & c_1 \\ a_2 & b_2 & c_2 \\ a_3 & b_3 & c_3 \end{bmatrix} \begin{bmatrix} X_S \\ Y_S \\ Z_S \end{bmatrix}. \qquad (2)$$

Here X_S, Y_S, and Z_S represent the accelerations measured in the sensor frame as described in (1); X_E, Y_E, and Z_E are the accelerations rotated into the earth coordinate frame; and the direction cosines for the above transformation are in terms of the Euler attitude angles (Anctil et al. 1994):

$$a_1 = \cos\theta \cos\psi$$
$$b_1 = \sin\varphi \sin\theta \cos\psi - \cos\varphi \sin\psi$$
$$c_1 = \cos\varphi \sin\theta \cos\psi + \sin\varphi \sin\psi$$
$$a_2 = \cos\theta \sin\psi$$
$$b_2 = \sin\varphi \sin\theta \sin\psi + \cos\varphi \cos\psi$$
$$c_2 = \cos\varphi \sin\theta \sin\psi - \sin\varphi \cos\psi$$
$$a_3 = -\sin\theta$$
$$b_3 = \sin\varphi \cos\theta$$
$$c_3 = \cos\varphi \cos\theta,$$

where the pitch θ is the rotation about the port–starboard axis of the buoy; the roll φ is the rotation about the bow–stern axis; and ψ is the heading of the buoy's bow, defined as magnetic compass degrees. The pitch is positive when the bow is up; the roll is positive when the starboard side is up. Once the accelerations have been rotated into the earth frame, the earth-referenced accelerations of the buoy are given by

$$A_x = -gX_E$$
$$A_y = -gY_E$$
$$A_z = g(1 - Z_E), \qquad (3)$$

where A_x, A_y, and A_z are the nongravitational accelerations along the earth oriented x, y, and z axes. Finally, we note that inverting (2) yields

$$\begin{bmatrix} X_S \\ Y_S \\ Z_S \end{bmatrix} = \begin{bmatrix} a_1 & a_2 & a_3 \\ b_1 & b_2 & b_3 \\ c_1 & c_2 & c_3 \end{bmatrix} \begin{bmatrix} X_E \\ Y_E \\ Z_E \end{bmatrix}. \qquad (4)$$

1) TILT CORRECTION

We describe five methods to calculate the heave, or vertical, acceleration time series from the accelerometer record. The first three methods assume that only a strapped-down, one-axis (1D) accelerometer is available, a typical setup for many older buoy designs. The fourth and fifth methods are based on a strapped-down, three-axis accelerometer, the design of some newer buoys. The first and fourth methods do not require any orientation data, whereas the other three methods require concurrent pitch, roll, and heading information. This provides a range of processing options that can be used depending on the motion sensor equipment installed in the buoy and the level of integration between individual sensors.

(i) Method I

The first method is used when strapped-down, 1D accelerometer data are available, but pitch and roll data are not. It computes the estimated deck relative acceleration by assuming the wave slopes φ and θ are small. Then (2) reduces to

$$X_E \cong X_S \cos\psi - Y_S \sin\psi$$
$$Y_E \cong X_S \sin\psi + Y_S \cos\psi$$
$$Z_E \cong Z_S,$$

and the estimated deck relative acceleration is

$$\hat{a}_z = g(1 - Z_S). \qquad (5)$$

If the wave buoy is heaving, but the deck remains level, then removing gravity from the accelerometer measurement is straightforward since in (1) $g_x = g_y = 0$ and $g_z = g$. If the buoy is pitching and rolling while it is heaving, then the component of gravity measured by the three orthogonal axes of the accelerometer is constantly changing. If the roll and pitch are sufficiently small (<10°), then to a first order approximation $g_x = g_y = 0$ and $g_z = g$ and (5) holds, though it will underestimate the wave heights; the error growing as the roll and pitch increase. If the pitch and roll are not small and the buoy is heeled over due to wind and current forcing, conditions expected to occur in storm events, then it will be shown that (5) overestimates the wave heights. In the absence of any sustained tilt, that is, heel, it can be theoretically shown that (5) underpredicts the actual wave heights.

(ii) Method II

It is important to realize that (5) is not the true deck relative acceleration because it does not properly account for the component of gravity measured by the z axis of the accelerometer. The second method computes the true deck relative acceleration by using the pitch and roll information to determine the component of gravity along the z axis of the accelerometer. Using (4) and $X_E = Y_E = 0$ g and $Z_E = 1$ g,

$$g_z = g \cos\varphi \cos\theta,$$

so that the true deck relative acceleration is

$$a_z = g(\cos\varphi \cos\theta - Z_S). \qquad (6)$$

Of course when the wave slopes become vanishingly small this reduces to (5).

(iii) Method III

The ideal estimate of wave heights should be derived from the earth-referenced vertical acceleration, not the deck relative acceleration. The deck relative acceleration, whether estimated (method I) or true (method II), is not a true estimate of the vertical acceleration of the wave field, particularly when the wave slopes are steep. The third method computes an estimate of the true earth-referenced vertical acceleration using the true deck relative acceleration, (6), and the pitch and roll information to orient the accelerations vertically in the earth reference frame. Using (2) and (6),

$$\hat{A}_z = c_3 a_Z = g(\cos\varphi \cos\theta - Z_s) \cos\varphi \cos\theta. \qquad (7)$$

Once again, when the wave slopes become vanishingly small this reduces to (5).

(iv) Method IV

The fourth method computes an estimate of the true earth-referenced vertical accelerations using the accelerations from all three axes, but not the pitch and roll information. This method is exact provided the horizontal accelerations of the buoy caused by waves are much smaller than the vertical accelerations. If $a_x = a_y = 0$ so that $X_E = Y_E = 0$, then the sensor measurements are

$$X_S = a_3 Z_E = -\sin\theta Z_E$$
$$Y_S = b_3 Z_E = \sin\varphi \cos\theta Z_E$$
$$Z_S = c_3 Z_E = \cos\varphi \cos\theta Z_E.$$

Summing the squares of the three accelerations shows that the magnitude of the three sensor accelerations is the earth-referenced z acceleration,

$$X_S^2 + Y_S^2 + Z_S^2 = \sin^2\theta Z_E^2 + \sin^2\varphi \cos^2\theta Z_E^2$$
$$+ \cos^2\varphi \cos^2\theta Z_E^2 = Z_E^2.$$

Therefore, from (4)

$$\hat{A}_z = g(1 - Z_E) = g(1 - \sqrt{X_S^2 + Y_S^2 + Z_S^2}). \quad (8)$$

Because the inertial response of the buoy to wave-induced horizontal accelerations is usually far smaller than it is to vertical accelerations, this method is quite accurate and only incurs errors when wave heights are large. This method was presented in Bender et al. (2008).

(v) Method V

The fifth method computes the true earth-referenced vertical acceleration. This method uses the accelerations from all three axes and the pitch and roll information to obtain the true earth-referenced vertical accelerations of the buoy. Using (2) and (3),

$$A_z = g(1 - Z_E) = g[1 - (a_3 X_s + b_3 Y_s + c_3 Z_s)]. \quad (9)$$

2) TIME SYNCHRONIZATION

We adjusted the pitch, roll, and heading data recorded by the Honeywell HMR digital compass to that of the Crossbow accelerometer data by correcting for the time lag between the pitch rate recorded by the Crossbow and the inferred pitch rate calculated using a five-point difference scheme from the compass pitch time series. The time lag was determined from the correlation between the two time series.

3) FILTERING

The time-lag-corrected acceleration data were then processed to remove outliers. The outliers were removed by first linearly detrending the data and then removing any value that exceeded 3 times the standard deviation. This typically accounted for less than 0.5% of the data. The data were then interpolated using cubic splines to a 4-Hz time base, which replaced any removed outliers. Finally, the data were processed through a Kalman filter to remove instrument and process noise. The Kalman filter is particularly useful because it estimates the state of a dynamic system from a series of noisy measurements. The level of filtering was guided by the desire to minimize the wave heights differences with NDBC's 42007 for a low-wave environment.

4) ACCELERATION SPECTRA

The acceleration wave spectra were determined by taking an FFT of the filtered, 4-Hz acceleration data.

Using 19.2 min of data, the data were segmented into seventeen 50% overlapping segments with 512 data points in each segment. A Kaiser–Bessel window based on the modified zero-order Bessel function of the first kind was applied to each segment to reduce spectral leakage. The Kaiser–Bessel window was used because it has very good dynamic range, is superior to most other windows with respect to selectivity, and uses an adjustable parameter beta ($\beta = 0.5$ in our case) to trade-off sidelobe energy for the main lobe. The FFT of the windowed segment was computed, corrected for the energy reduction due to the windowing, and the one-sided power spectra calculated. Each of the 17 power spectra were then averaged to obtain the final acceleration wave spectra.

5) FREQUENCY DOMAIN FILTER

The next processing step applied a frequency domain filter to the acceleration spectra to remove low-frequency noise. We utilized a modification of the empirical noise correction of Lang (1987), which establishes a noise estimate and then removes that noise in a linearly decreasing manner between a lower (0.05 Hz) and upper (0.15 Hz) frequency. We determined the noise estimate to be the product of the mean spectral density between 0.01 and 0.05 Hz and the slope of the noise correction factor S_{nc} to be 20.

6) DISPLACEMENT SPECTRA

Finally, the noise-corrected acceleration spectra were converted to the displacement spectra by dividing by the frequency to the fourth power. The heave response amplitude operator used by NDBC for its 3-m discus buoys was applied. The significant wave height, peak period, and mean wave period were determined from the displacement spectra using the definitions provided on the NDBC Web site (NDBC 2008; available online at http://www.ndbc.noaa.gov/).

7) VERIFICATION

To verify the proceeding steps were a reasonable and accurate means of determining the displacement spectra, we extensively tested the processing algorithms using a simulated wave field derived from a depth-limited Joint North Sea Wave Project (JONSWAP) spectra, determining the acceleration time series from the displacement time series. We determined there were minor differences between the starting and reconstructed spectra, and no difference in the significant wave height, peak period, or mean period.

b. Global positioning service

The GPS-derived displacement time series is a measure of the displacement of the phase center of the buoy's

GPS antenna, not the geometric center of the buoy where the accelerometer sensor is located. The antenna is located approximately 380 cm above mean water level, offset by approximately 60 cm from the center of the buoy, and at a clockwise angle of 30° relative to buoy north. As a result of this lever arm, the displacement data reflects a combination of the heave of the buoy and its pitch and roll. The GPS measurements were not tilt corrected because of still to be resolved synchronization issues between the GPS data and the Honeywell HMR pitch and roll data.

The 1-Hz displacement time series was processed as a displacement spectrum, yielding the significant wave height, mean period, and peak period. All of the processing steps for doing this are identical to the accelerometer methods described previously, with the exception of needing to apply the frequency domain filter. Unlike the acceleration wave spectra, the displacement spectra do need to be corrected for spurious low-frequency noise introduced by dividing by the frequency to the fourth.

4. Results

a. Estimated deck relative acceleration

NOAA's NDBC 3-m discus buoy 42007 was deployed approximately 7 nm to the west–northwest of the USM buoy, near the 14-m isobath (Fig. 1). We retrieved hourly one-dimensional spectral estimates, the significant wave height, the peak period, and the mean period from the NDBC Web site for this buoy for all of 2005. Buoy 42007 is equipped with the data acquisition and control telemetry (DACT) payload (NDBC 2003). The DACT payload contains a two-axis magnetometer for measuring buoy slope and heading and a fixed, one-axis accelerometer for measuring buoy heave. The vertical acceleration of the buoy hull is measured with a Schaevitz LSOC-30 inclinometer (NOAA 2009). The LSOC-30 inclinometer is a solid-state, closed-loop, force-balance, gravity-referenced tilt sensor that measures the tilt, up to 30°, from the output of a vertically oriented accelerometer. The sensor is used in the buoy as an accelerometer sensing accelerations along the mast axis. The sensed accelerations contain the components of gravity that are removed using method I to obtain the mast acceleration. (T. Mettlach 2009, personal communication). It is the method implied in Earle and Bush (1982) that leads to their Eq. (23) for deck relative acceleration caused by waves.

The heave acceleration from the z acceleration axis of the Crossbow IMU400CC sensor was processed with method I to obtain comparable significant wave heights, peak periods, and mean periods. The time series of significant wave heights is compared to NDBC buoy 42007
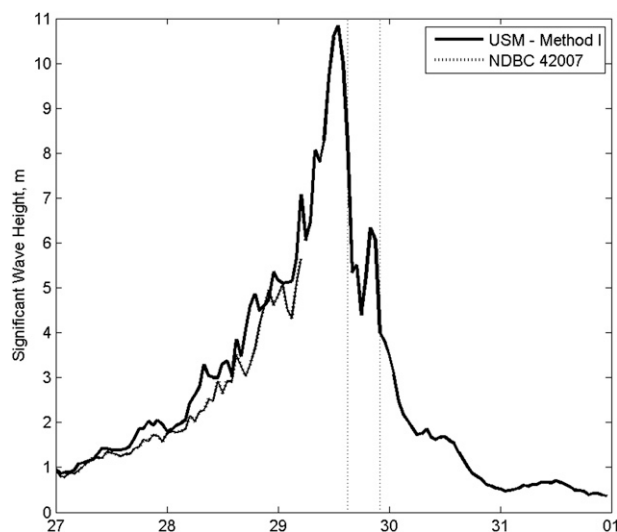

FIG. 3. Time series of significant wave heights for the estimated deck relative accelerations (method I) vs NDBC 42007 from 27 through 31 Aug. See text for additional details. The vertical dotted lines denote the time period the USM buoy was moving. The NDBC buoy data ceases after 0500 UTC 29 Aug.

in Fig. 3. There is little difference in wave heights less than 1.0 m (not shown), but for wave heights greater than 1.0 m the NDBC buoy tends to be lower. The maximum wave height of 10.73 m for the USM buoy occurred at 1300 UTC 29 August 2005. Figure 4 presents the scatterplots of USM versus NDBC significant wave heights; it does not include any data during the period the buoy was moving. The symmetric regression linear fit (Taagepera 2009) has a slope of 0.886, implying that the NDBC heights are underestimated by 11.4% relative to the USM method I heights. Table 1 shows a matrix of statistical parameters for this comparison. The scatter index, defined as the standard deviation of the height differences divided by the mean of the USM method I heights, is 23.7%, which is relatively high. The rmse is 0.226 m and the r^2 correlation is 0.984. These differences could be due to differences in the local sea state, differences in the water depth, differences in the processing strategies, or some combination of all three. The high r^2 correlation suggests both buoys are measuring the same physical process, but the other statistics suggest that there are differences in the processing strategies.

b. True deck relative accelerations versus GPS

The true deck relative acceleration (method II) gives the vertical motion of the buoy deck, which is most similar to the motion of the GPS antenna. Using the true deck relative acceleration and the GPS displacement data, we computed significant wave heights, peak periods, and mean periods. The time series of resulting
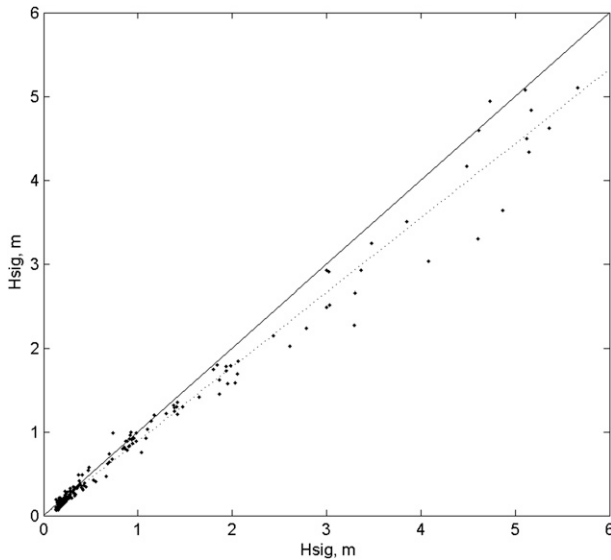
FIG. 4. Scatterplot of significant wave height for the estimated deck relative accelerations (method I, horizontal axes) and NDBC 42007 (vertical axes). The line of perfect agreement is shown as a solid line and the symmetric regression linear fit (slope = 0.886) as a dotted line.

TABLE 1. Statistical parameters for significant wave height scatterplots.

Comparison	Slope	Scatter index (%)	RMSE (m)	r^2 corr
I vs 42007	0.886	23.7	0.226	0.984
II vs GPS	1.014	5.4	0.065	0.998
I vs V	1.263	44.9	0.496	0.969
II vs V	1.052	8.8	0.098	0.998
GPS vs V	1.039	7.1	0.086	0.998
III vs V	1.010	2.3	0.025	1.000
IV vs V	0.974	4.82	0.053	0.999

wave heights. For the estimated deck relative acceleration data (method I), the largest difference occurred at 1300 UTC 29 August 2005, when the wave height reached 10.84 m and the buoy heel was 18.2°. For the true vertical acceleration data (method V), the corresponding maximum wave height is 6.94 m—the peak period and mean period are unchanged. This reduction in the peak wave height is a direct result of using method V to account for the buoy heel. A comparison of the two displacement spectra at 1300 UTC 29 August 2005 is shown in Fig. 8. It illustrates that the energy is primarily reduced in the region near the peak frequency, where the wave energy is at a maximum. The individual peaks are not shifted in frequency. This suggests that swell waves are the most likely to be overestimated when the buoy is heeled. The scatterplot of significant wave height is shown in Fig. 9 and, as before, does not include

significant wave heights is shown in Fig. 5. Up until the time the GPS base station went offline, the two wave heights show exceptional agreement. The maximum wave height of 8.17 m occurred at 1700 UTC 29 August 2005. The scatterplot of significant wave height is shown in Fig. 6; it does not include any data during the period the buoy was moving. The symmetric regression linear fit has a slope of 1.014, a scatter index of 5.4%, an rms error of 0.065 m, and an r^2 correlation of 0.998. We can conclude with fairly high confidence that the vertical displacement of the GPS antenna and the true deck relative acceleration are measuring the same vertical motion. Given the amount of processing needed to generate the GPS displacement time series, as well as the unique differences between an accelerometer and a GPS receiver, we find this level of agreement remarkable.

c. Estimated deck relative acceleration versus true vertical acceleration

The estimated deck relative acceleration (method I) is the method most commonly used with a strapped-down, 1D accelerometer to determine the wave heights. Figure 7 shows the time series of wave heights of the true vertical acceleration (method V, for which a 3D accelerometer and pitch, roll, and heading data are required) compared to method I. There is no apparent difference in wave heights less than 3 m, for which the buoy heel is small, but there is a marked difference in the larger
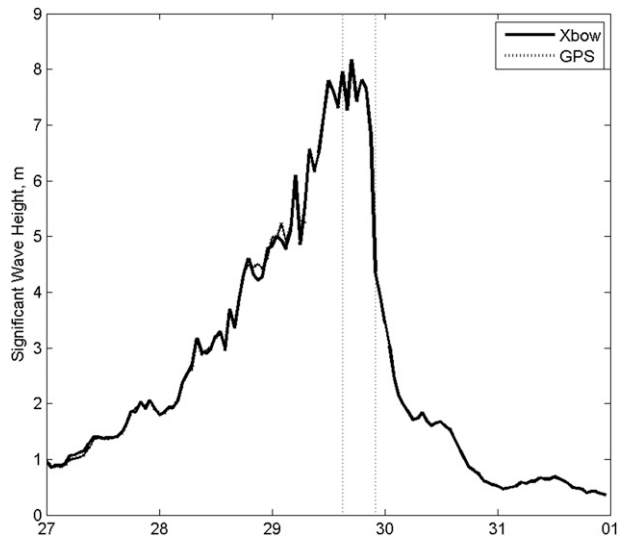

FIG. 5. Time series of significant wave heights for the true deck relative accelerations (method II, labeled as Xbow) vs the GPS displacements (labeled as GPS) from 27 through 31 Aug. The vertical dotted lines denote the time period the buoy was moving. The GPS data ceases after 0727 UTC 29 Aug. See text for additional details.
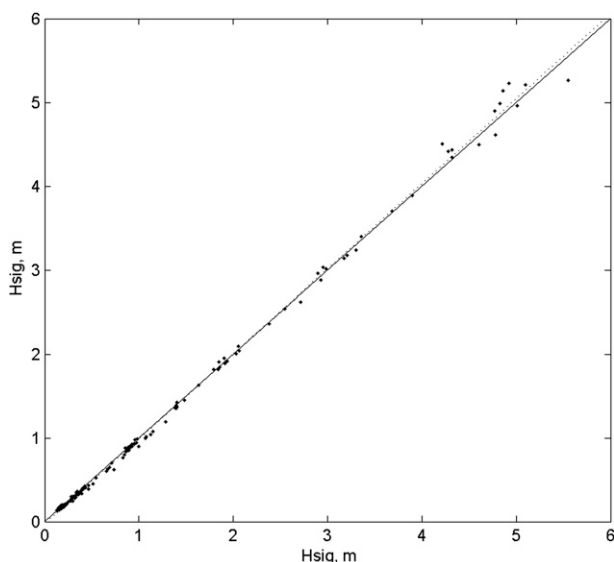
FIG. 6. Scatterplot of significant wave height for the true deck relative accelerations (method II, horizontal axes) vs GPS displacement (vertical axes). The line of perfect agreement is shown as a solid line and the symmetric regression linear fit (slope = 1.014) as a dotted line.
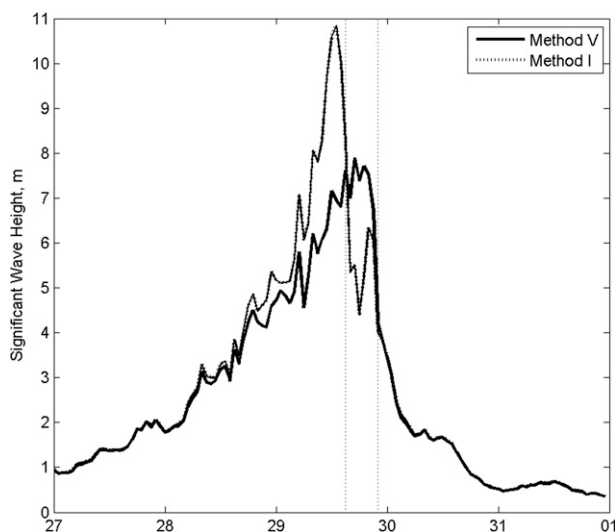

FIG. 7. Time series of significant wave heights for estimated deck relative acceleration (method I) vs true vertical acceleration (method V) from 27 through 31 Aug. The vertical dotted lines denote the time period the buoy was moving. See text for additional details.

any data during the period the buoy was moving. The symmetric regression linear fit has a slope of 1.263, meaning the deck relative accelerations (method I) overestimates the wave heights by an average of 26%. For large wave heights the linear regression breaks down and the overestimation of wave heights becomes greater than 26%. Table 1 lists the scatter index, the rms error, and the r^2 correlation.

d. True deck relative acceleration versus true vertical acceleration

The true deck relative acceleration (method II) uses pitch and roll information to remove the component of gravity along the z axis of the accelerometer. As such, it is not constrained to small tilts, as method I is, but it is valid when the pitch and roll become large. In the case of a directional buoy with a strapped-down, 1D acceler-ometer, this would be a method for dealing with buoy heel. Figure 10 shows the time series of wave heights of the true deck relative acceleration (method II) com-pared to the true vertical acceleration (method V). There is no apparent difference in wave heights less than 3 m, but above 5 m method II slightly overestimates the wave heights. For the true deck relative acceleration data, the maximum wave height of 8.17 m occurred at 1700 UTC 29 August 2005. For the true vertical accel-erations data, the maximum wave height of 7.90 m oc-curs at the same time. The scatterplot of significant wave height is shown in Fig. 11; it does not include any data

during the period the buoy was moving. The symmetric regression linear fit has a slope of 1.052. It is only above 5 m that the 5% overestimation becomes apparent. Table 1 lists the scatter index, the rms error, and the r^2 correlation.

e. Estimated vertical acceleration versus true vertical acceleration

The accelerations for determining wave heights should be the earth-referenced vertical acceleration (i.e., aligned with the gravity vector) and not the deck-referenced ac-celeration. These vertical accelerations can be estimated using a strapped-down, 1D accelerometer along with pitch and roll information. This method, method III, is an improvement over method II because it provides a better estimate of the true wave heights while using the same data available to method II. In the case of a di-rectional buoy with a strapped-down, 1D accelerometer, this is the best method for dealing with buoy heel. Figure 12 compares the wave heights determined from the true vertical acceleration (method V) to the wave heights from the estimated vertical acceleration (method III). There is virtually no visual difference in wave heights less than 6 m and only minor differences in larger wave heights. For the estimated vertical acceleration data, the maximum wave height of 7.67 m occurred at 1500 UTC 29 August 2005 when the buoy was moving to the south-east. For the true vertical accelerations data the maximum wave height of 7.90 m is slightly higher. The scatterplot of significant wave height, using the data when the buoy
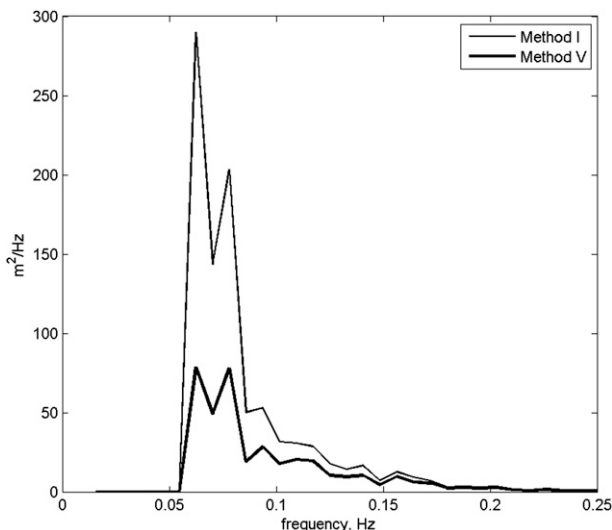
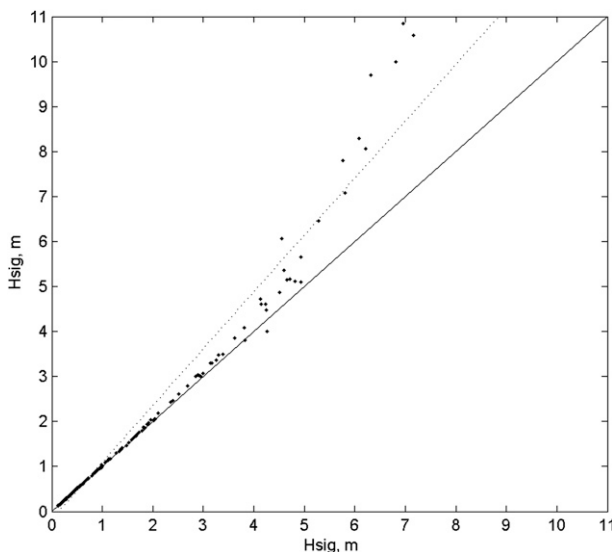FIG. 8. Comparison of displacement spectra at 1300 UTC
29 Aug 2005.

FIG. 9. Scatterplot of significant wave height for the true vertical acceleration (method V, horizontal axes) vs the estimated deck relative acceleration (method I, vertical axes). The plot does not include data when the buoy was moving. The line of perfect agreement is shown as a solid line and the symmetric regression linear fit (slope = 1.263) as a dotted line.

was not moving, is shown in Fig. 13. The symmetric regression linear fit has a slope of 1.010, meaning the estimated vertical accelerations overestimate the true vertical accelerations on average by 1%. Table 1 lists the scatter index, the rms error, and the r^2 correlation, which clearly indicates this method is superior to the others.

f. Horizontal accelerations

The 1% difference in wave heights between the estimated vertical acceleration, which is based on a strapped-down, 1D accelerometer, and the true vertical acceleration, which utilizes the accelerations in all three orthogonal axes, is probably due to wave-induced horizontal accelerations. Longuet-Higgins (1986), in his work on the Eulerian and Lagrangian aspects of surface waves, showed that in progressive deep-water gravity waves the horizontal accelerations generally exceed the vertical accelerations. If the buoy were a true particle following platform (i.e., Lagrangian), then the strapped-down, z-axis accelerometer would measure wave-induced horizontal accelerations whenever the buoy was tilted. A pitch and roll buoy is not a true Lagrangian platform but neither is it a true Eulerian platform. If a wave buoy were truly Eulerian, then it would not experience any horizontal accelerations, yet its strapped-down accelerometer would still measure the component of the wave's vertical acceleration in the x and y axes as pseudohorizontal accelerations whenever the buoy was tilted. A transformation from the sensor frame to the earth coordinate frame would show these horizontal accelerations to be no more than the noise of the instrument. If the buoy were truly Lagrangian, then it would follow a particle on the surface

and experience significant horizontal accelerations. A transformation from the sensor frame to the earth coordinate frame would show these horizontal accelerations to be on the order of the vertical accelerations.

For low waves the USM 3-m discus buoy responded in a highly Eulerian manner. This is most clearly seen in the histogram of accelerations at 0000 UTC 27 August 2005 as shown in Fig. 14. Once the x, y, and z accelerations are transformed from the sensor frame to the earth coordinate frame it is seen that the horizontal accelerations are within the noise of the instrument. For high waves the buoy responds in a less Eulerian manner but neither is it truly Lagrangian. This is seen in the histogram of accelerations at 1300 UTC 29 August 2005, as shown in Fig. 15. The measured x, y, and z accelerations are clearly offset by the heel of the buoy. Once the x, y, and z accelerations are transformed from the sensor frame to the earth coordinate frame it is seen that the offset disappears and the horizontal accelerations are normally distributed about zero. If one roughly estimates the noise of the instrument based on the low wave results at 0000 UTC 27 August 2005, then the tilt-corrected horizontal accelerations are statistically significant. This implies that wave-induced horizontal accelerations are affecting the motion of the buoy, but because the horizontal accelerations are not of the order of the vertical (Longuet-Higgins 1985, 1986), the buoy is not responding as an ideal Lagrangian platform but as a semi-Lagrangian
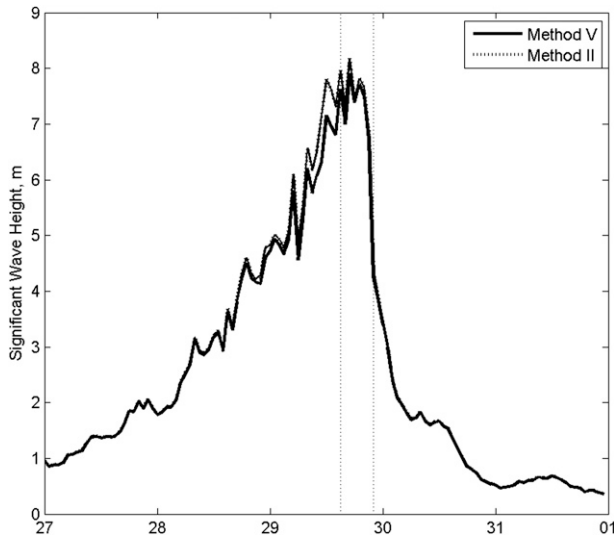
FIG. 10. Time series of significant wave heights for true deck relative acceleration (method II) vs true vertical acceleration (method V) from 27 through 31 Aug. The vertical dotted lines denote the time period the buoy was moving. See text for additional details.
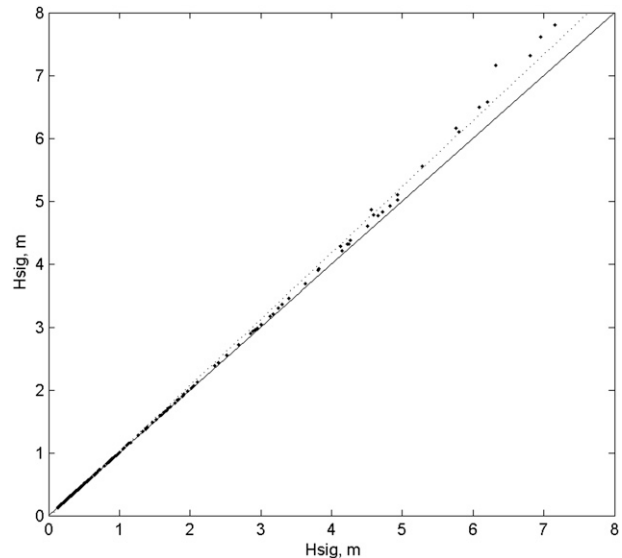

FIG. 11. Scatterplot of significant wave height for the true vertical acceleration (method V, horizontal axes) vs the true deck relative acceleration (method II, vertical axes). The plot does not include data when the buoy was moving. The line of perfect agreement is shown as a solid line and the symmetric regression linear fit (slope = 1.052) as a dotted line.

platform. The heel of the buoy combined with the wave-induced horizontal accelerations means that the measured z accelerations from a strapped-down accelerometer are overestimated and must be tilt corrected.

g. Buoy heel

The heel of the buoy, and in particular its orientation relative to the wind and swell direction, controls whether method I over- or underestimates the wave heights. Figure 7 shows that the wave heights were overestimated when the buoy was stationary but were underestimated during the period when the buoy was moving to the southeast. To explain this behavior, a time series record of the buoy heel was constructed from the 4-Hz pitch and roll data. The 20-min-averaged pitch and roll data were combined with the azimuth data to obtain a geographically referenced east–west (EW) heel, corresponding to the roll, and a north–south (NS) heel, corresponding to the pitch. Hence, for the purposes of this discussion a reference to the east axis of the buoy does not refer to the starboard side of the buoy, but to the axis of the buoy that is aligned along the compass direction of west to east. The east–west heel is positive for upward motion of the east axis of the buoy. The north–south heel is positive for upward motion of the north axis of the buoy. A wind from the east, defined as positive, would act on the superstructure of the buoy and rotate the buoy about its center of momentum, causing the eastward orientation of the buoy to heel upward, that is, positive. On the other hand, if the buoy mooring was scoped out to the west of

the buoy (buoy set east of its anchor) because the buoy is drifting to the east, this would cause the east axis of the buoy to heel down. A wind from the south, defined as negative, would result in the north axis of the buoy heeling downward, that is, negative. If the buoy mooring was scoped out to the north of the buoy (buoy set south of its anchor), this would cause the north axis of the buoy to heel upward.

In Fig. 16, we show the EW and NS heel of the buoy, averaged over 20 min; the associated wind speed, averaged over the first 10 min of the pitch and roll sampling period; and the difference in significant wave heights, defined as the estimated deck relative accelerations (method I) minus the true vertical accelerations (method IV). As seen from Fig. 16, the buoy heel and wind speed follow very closely when the buoy is stationary. The easterly wind causes a positive EW heel and the southerly wind causes a negative NS heel. The overestimation in significant wave height is at its largest when the NS heel is most negative. But when the buoy is moving to the south–southeast, the mooring is presumably scoped out to the north–northwest and causes two things to happen. The east axis of the buoy heels down more than expected for the velocity of the easterly wind and the NS heel is less than expected. This corresponds to the rapid reversal in the bias of the significant wave heights, where the method I heights are now less than the method V heights. A model confirms this behavior.
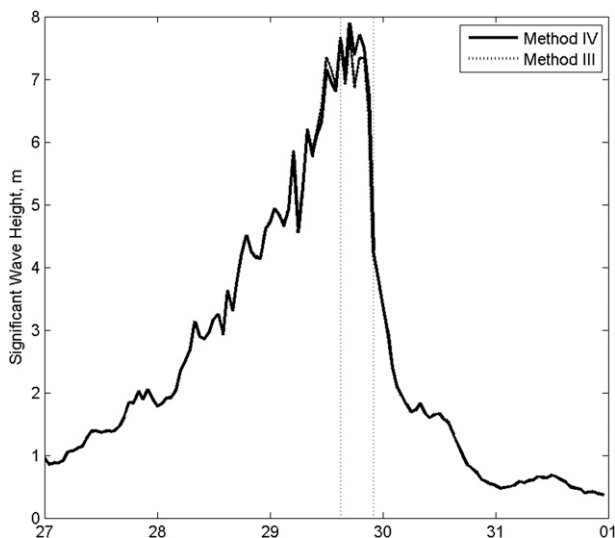
FIG. 12. Time series of significant wave heights for estimated true vertical acceleration (method III) vs true vertical acceleration (method V) from 27 through 31 Aug. The vertical dotted lines denote the time period the buoy was moving. See text for additional details.
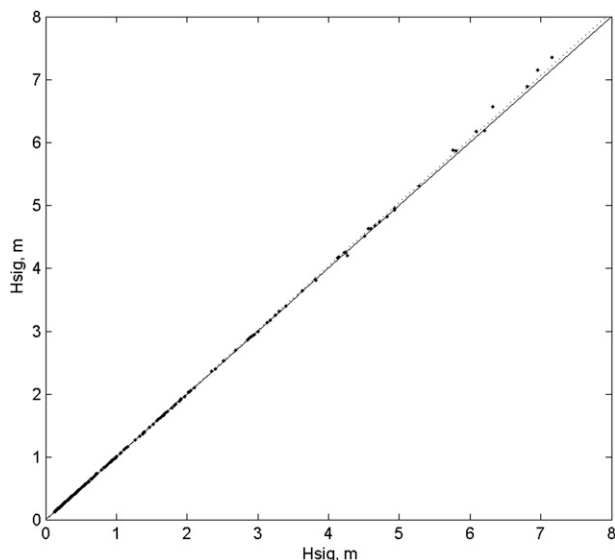

FIG. 13. Scatterplot of significant wave height for the true vertical acceleration (method V, horizontal axes) vs the estimated deck relative acceleration (method III, vertical axes). The plot does not include data when the buoy was moving. The line of perfect agreement is shown as a solid line and the symmetric regression linear fit (slope = 1.010) as a dotted line.

h. Empirical correction

Correcting a buoy's wave heights for buoy heel, when the raw heave and tilt data are not available, is somewhat problematic. But in the case of the USM buoy, where there is a good correlation between wind velocity and buoy heel, we can explore what that empirical correction might look like. Following 1400 UTC 29 August 2005 the buoy was subjected to considerable mooring forces as it was moved by the relaxing storm surge. At this point the heel was no longer primarily due to the wind. Figure 17 shows the empirical relationship between the heel of the buoy, the wind speed, and the differences in significant wave heights. To ensure that the wind is the major factor in determining the buoy's heel, not excessive forces from the mooring, only data from 20 August up to the point the buoy began moving are used. For wind speeds less than 7.5 m s^{-1}, corresponding to a heel less than ~3°, there is no difference in whether the wave heights are tilt corrected or are not tilt corrected. But above 7.5 m s^{-1}, a quadratic relationship exists between heel, wind speed, and percent overestimation. This is a consequence of the fact that wind force is proportional to the square of the velocity, and it is the force of the wind acting on the superstructure that contributes to the buoy heel. For the specific case of the USM buoy, Fig. 17 provides a straightforward means of empirically correcting the wave heights using the wind speed alone; however, how this relationship would be modified for a different buoy, a different water depth, and a different wave environment is problematic.

5. Discussion

In the most widely used method (method I) for a buoy with a strapped-down, 1D accelerometer, wave heights are computed from the deck relative z-axis accelerations. Gravity is removed by assuming that the pitch and roll of the buoy is small, implying that the orientation of the accelerometer is nearly vertical. In the presence of hurricane conditions when the buoy had a heel of 18°, the accelerometer was not vertical and wave heights computed in this manner were inaccurate. To account for the buoy heel, pitch and roll data are imperative. A directional buoy with a strapped-down, 1D accelerometer presumably has this information on board. The second method (method II) uses the orientation data to remove the component of gravity from the deck relative z-axis accelerations. This is most similar to the motion of the GPS antenna and was shown to be surprisingly identical to the GPS displacement data. The method overestimates wave heights by 5%; it can be improved to 1% with no additional data. The third method (method III) uses the orientation data to obtain a very accurate estimate of the vertical acceleration, on the basis that the accelerations for determining wave heights should be the earth-referenced vertical acceleration and not the deck-referenced acceleration used in method II. The fourth method (method IV), which is described elsewhere (Bender et al. 2008), is exact provided the horizontal accelerations are much smaller than the vertical. The
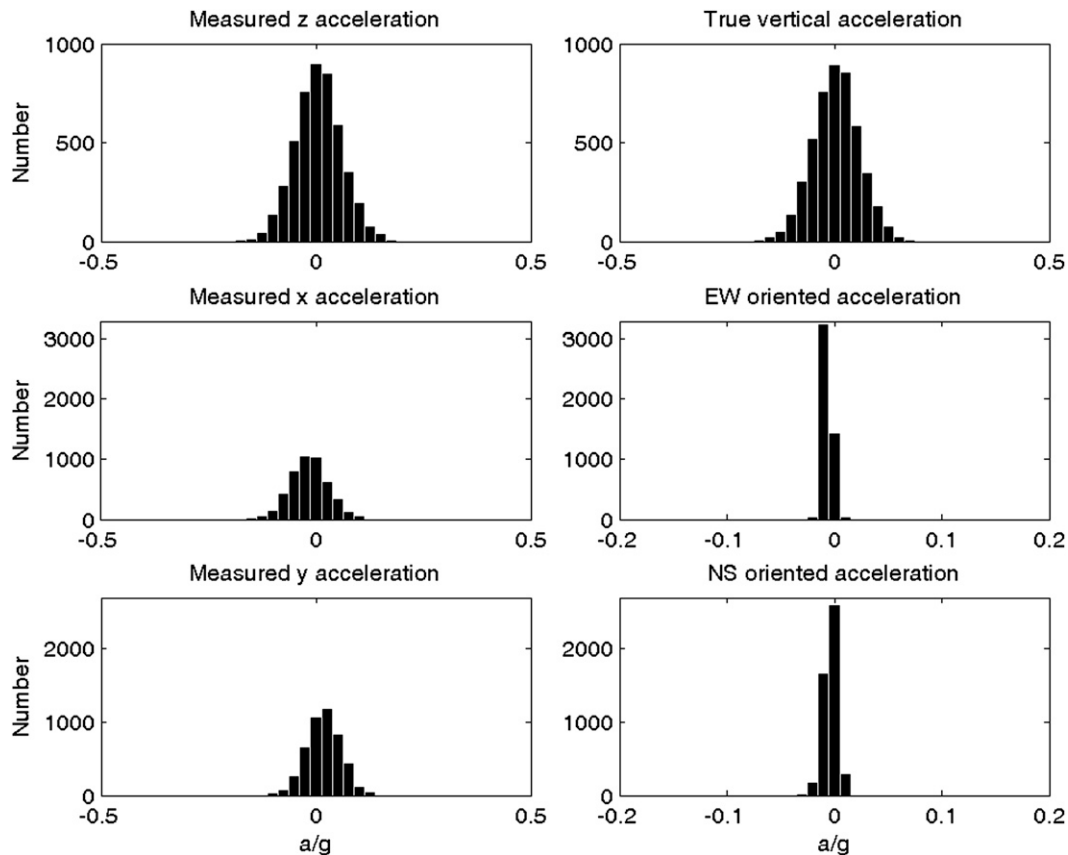
FIG. 14. Histogram of the orthogonal accelerations at 0000 UTC 27 Aug 2005. The significant wave height for the measured z acceleration (method I) is 0.954 m and for the true vertical acceleration (method V) it is 0.957 m. The earth-referenced horizontal accelerations are simply noise.

fifth method (method V) uses the acceleration from all three axes and the pitch and roll information to obtain the earth-referenced vertical acceleration of the buoy. It accounts for any horizontal acceleration that may be present and, consequently, is the most accurate means of determining wave heights.

a. Noise correction filter

The measurement of the acceleration of a floating surface buoy has been used as an indirect method for measuring wave height and direction since at least the mid-1950s (Barber 1946; M. S. Longuet-Higgins 1946, unpublished manuscript; Kinsman 1965). Tucker (1956, 1959) was the first to recognize that the accuracy of wave measurements made with a strapped-down, 1D accelerometer could be different from those made with a vertically stabilized accelerometer. He derived a theoretical expression for the error signal in using a fixed accelerometer and found that the spectrum of the error signal rose steeply at very low frequencies and increased with the sea state. The errors were comparable to the wave's spectral energy for frequencies less than 0.04 Hz, frequencies

that were quite rare even for swell in the Pacific. Tucker concluded that if a high-pass filter was used to remove the low-frequency components, then the errors were probably not serious for most purposes. This is the approach taken by NDBC (Burdette 1978; Steele et al. 1978; Steele and Earle 1979; Earle and Bush 1982; Earle et al. 1984; Lang 1987; Bouchard et al. 2009).

The use of a noise correction factor to correct for the spurious energy introduced by a single-axis, hull-fixed accelerometer is effective in efficiently eliminating extremely low-frequency "noise" that is not real. But in the case of a sustained buoy heel, usually occurring during storms when wave heights are already high, it masks how the heel of the buoy can dramatically influence the measured significant wave height. The future use of a noise correction filter on buoys with a three-axis accelerometer should be reevaluated and the filter's level of attenuation be adjusted to remove only the electronic and digitization noise. Furthermore, using an autocovariance estimate to determine the acceleration spectra allows one to eliminate frequency bins at very low frequencies, where no real wave energy is expected to exist.
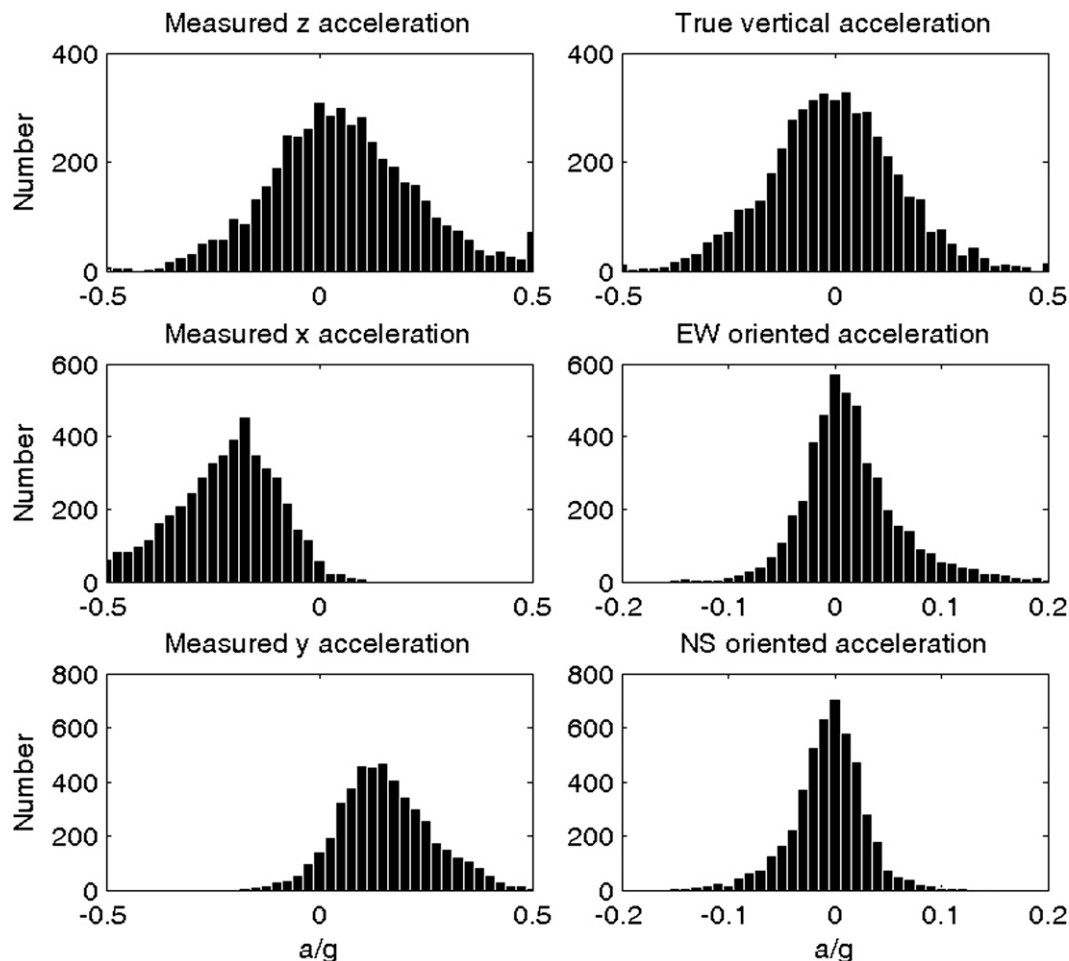
FIG. 15. Histogram of the orthogonal accelerations at 1300 UTC 29 Aug 2005. The significant wave height for the measured z acceleration (method I) is 10.84 m and for the true vertical acceleration (method V) it is 6.95 m.

b. Wave model validation

Significant wave heights determined from pitch and roll buoys are regularly used to validate numerical ocean wave model results. For example, Forristall (2007) compared hindcasts using Oceanweather's standard proprietary product for the Gulf of Mexico against wave measurements recorded during major hurricanes of the last few years. The hindcast wave heights for buoy 42040 during the passage of both Ivan and Katrina were underestimated compared to the buoy measurements. Buoy 42040 is a 3-m discus buoy with a fixed accelerometer; therefore, the failure to tilt correct could account for the difference. In contrast, the hindcast wave heights for buoy 42001 during the passage of Katrina were overestimated compared to the recorded buoy height. Buoy 42001 is a 12-m discus buoy and during Katrina it was equipped with a Hippy 40 (Forristall 2007). Failure to tilt correct should not account for the difference because

the accelerometer is vertically stabilized. But what the difference does suggest is that if the wave model had been tuned to match measured wave heights, and some of those wave heights came from pitch and roll buoys with single-axis fixed accelerometers that were not tilt corrected, then it is possible the wave model was tuned too high. If that was the case, then it would be reasonable to expect the wave heights from a vertically stabilized accelerometer to be lower than the model results.

The differences between model and hindcast suggests the validation of a numerical ocean wave model using wave heights from a heave, pitch and roll buoy should be considered cautiously. What may be a better approach is to "convert" the spectral model data into a pseudobuoy record. In other words, the spectral wave model data needs to first be processed like it was acquired by a pitch and roll buoy and then compared to the observational data. The displacement spectra from the model could be sampled as a Monte Carlo distribution of wave amplitudes
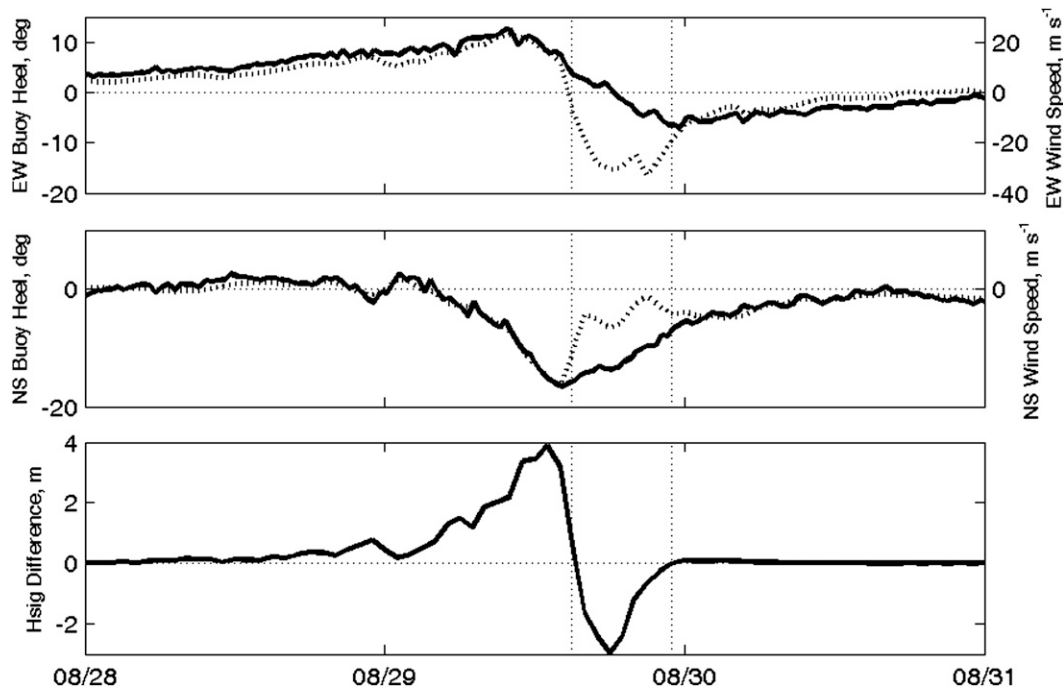
FIG. 16. (top) A comparison of the buoy heel and the wind speed in the east–west direction; (middle) the buoy heel and the wind speed in the north–south direction; (bottom) the significant wave height differences. In (top) and (middle) the dashed line is buoy heel and the solid line is the wind speed. The two vertical dashed lines shown in all three panels denote the period in which the buoy moved.

versus wave period and then converted to an ensemble of simulated acceleration time series. Knowing details about the buoy's payload package and its processing strategy, as well as accounting for its heel due to wind forcing, a pseudo–buoy wave height time series could be created. This could then be compared to the model results, in essence comparing apples against apples. This should be undertaken even if the accelerometer is vertically stabilized. The processing strategy of converting a limited period (typically 20 min), discrete (1–2 Hz) time series of accelerations through the steps of filtering and fast Fourier transform, followed by the removal of spurious low-frequency noise and the application of the heave amplitude transfer function, is not expected to yield the same displacement spectra as the model.

c. Mooring influence

Finally, it is reasonable to postulate that the all-chain catenary mooring for the USM buoy could have been scoped out during the 8 h it was dragged to the southeast. It is also possible that the mud seafloor became so highly fluidized by the large waves that the anchor itself became partially or fully suspended and the mooring may not have been fully scoped out. In either case, how the mooring affects the ability of a large reserve buoyancy discus buoy to respond to the wave field is a complex

question that cannot be answered here. One could argue that the wave heights, corrected or not corrected for tilt, may have been biased low during the period the buoy was moving. However, the deviation in nontilt-corrected and tilt-corrected wave heights was seen even before the buoy was dragged from its deployment location by the force of the relaxing storm surge. At the point at which the buoy begin to move to the southeast, 1400 UTC 29 August, the method I significant wave height had decreased from its peak of 10.73 to 9.89 m. This compares to the method IV wave height of 6.69 m. This is a difference of 3.20 m or a wave height that is 48% higher if tilt correction is not accounted for.

6. Conclusions

Computing wave heights from an accelerometer record assumes one has employed a means for removing the measurement of gravity from the data because any accelerometer experiences an offset due to gravity. More often than not this information is unavailable to anyone accessing archived wave height data from discus buoys. In this paper, we have attempted to show why this is important by creating a logical progression of steps, or methods, for gravity removal that are increasingly more complex—and consequently more expensive—but more
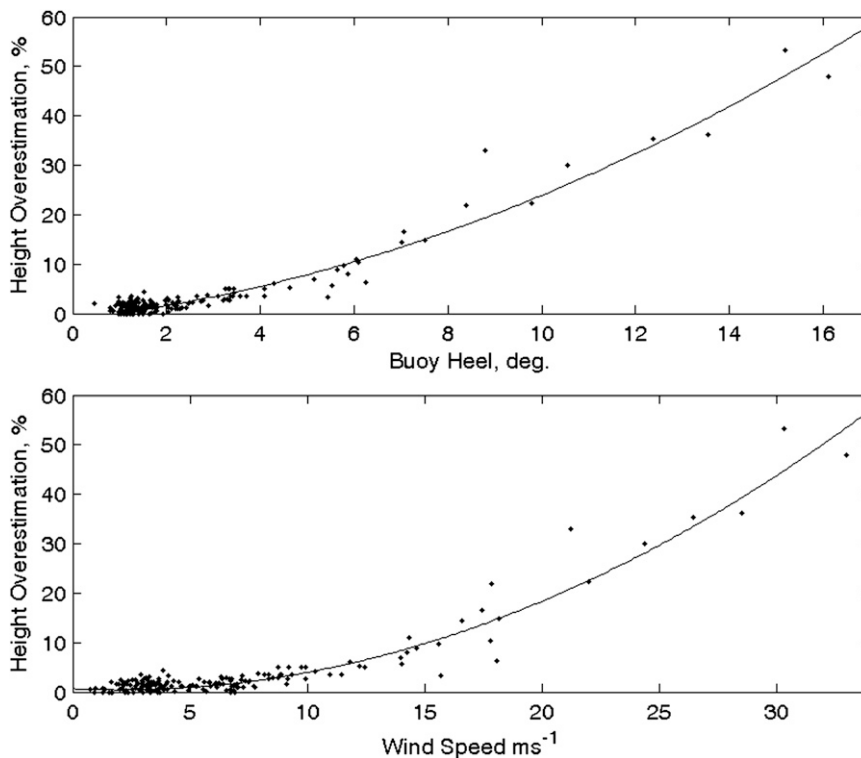
FIG. 17. Empirical relationship between the heel of the buoy, the wind speed, and the percent over prediction in wave heights, when the wind is the primary force acting on the USM 3-m discus buoy.

accurate. The primary conclusion is that the standard method of deriving wave heights from a strapped-down, 1D accelerometer is inaccurate when the buoy is subjected to a sustained heel that could be present when the waves are large. This is of particular importance to those interested in wave height observations under extreme conditions such as hurricanes.

We compared five different methods for determining significant wave heights from a heave–pitch–roll buoy, four methods using accelerometer measurements, and one method using vertical displacement from GPS measurements. The comparison between the GPS measurements and the deck relative accelerations are remarkably consistent, especially considering the two different and independent data sources and processing methods. As long as the buoy is not heeled excessively, less than ~1°, then any of the five methods give comparable results. It is only when the heel of the buoy exceeds 10° that differences in the five methods are seen—the largest being seen in the method most commonly used for correcting a strapped-down, 1D accelerometer.

The potential for the heel of a discus buoy to bias the measured wave heights must be understood when using a fixed, one-axis accelerometer. This is particularly important when the buoy is heeled over during the wave

sampling period, a condition that can be expected to occur when the wind speeds are high, when wave heights are correspondingly high, and obtaining accurate wave information is most critical. What we demonstrate in this paper is that the larger the heel, the greater the deviation in wave heights one can expect if the heel is not corrected for. A simple means of viewing this can be explained with an accelerometer that reads a -1 g (z axis positive down) when the accelerometer is stable. When installed on a pitch and roll buoy, a constant heel results in a positive offset of the accelerometer's z-axis component of gravity. The standard conversion to a deck relative acceleration, that is, add 1 g to the z-axis measurements, simply means that the hull-induced offset is seen as a dc upward acceleration superimposed on an ac component. When the heel is large, the amplitude of the ac component can be very large, leading to a significant overestimation of the wave heights.

REFERENCES

Anctil, F., M. A. Donelan, W. D. Drennan, and H. C. Graber, 1994: Eddy-correlation measurements of air-sea fluxes from a discus buoy. *J. Atmos. Oceanic Technol.,* **11,** 1144–1150.

Barber, N. F., 1946: Measurements of sea conditions by the motion of a floating buoy. Admiralty Research Laboratory Tech. Note A.R.L./103.40/N.2/w., 8 pp.

Bender, L. C., N. L. Guinasso, J. N. Walpert, L. L. Lee, R. D. Martin, R. D. Hetland, S. K. Baum, and M. K. Howard, 2007: Development, operation and results from the Texas Automated Buoy System. *Gulf Mex. Sci.,* **25,** 33–60.

——, ——, ——, and S. D. Howden, 2008: Wave heights from a 3-m discus buoy during Hurricane Katrina. *Proc. MTS/IEEE Oceans 2008 Conf.,* Quebec City, QC, Canada, Institute of Electrical and Electronics Engineers, 1–7.

Bouchard, R., C.-C. Teng, R. Riley, and W. H. Burnett, 2009: Status of and plans for the wave measurements program at NOAA's National Data Buoy Center. *Proc. 11th Int. Workshop on Wave Hindcasting and Forecasting,* Halifax, NS, Canada, Environment Canada, digital media. [Available online at http://www.waveworkshop.org/11thWaves/ProgramFrameset.htm.]

Burdette, E. L., 1978: The comparison of discus buoy wave spectra produced by buoy-fixed and vertically stabilized accelerometers. *Proc. MTS/IEEE Oceans 1978 Conf.,* Washington, DC, Institute of Electrical and Electronics Engineers, 327–332.

Dodd, D., S. Bisnath, and S. Howden, 2006: Implementation of ionosphere and troposphere models for high-precision GPS positioning of a buoy during Hurricane Katrina. *Proc. 19th Int. Technical Meeting of the Satellite Division of the Institute of Navigation ION GNSS,* Fort Worth, TX, The Institute of Navigation, 2006–2016.

Earle, M. D., and K. A. Bush, 1982: Strapped-down accelerometer effects on NDBO wave measurements. *Proc. MTS/IEEE Oceans 1982 Conf.,* New York, NY, Institute of Electrical and Electronics Engineers, 838–848.

——, K. E. Steele, and Y. L. Hsu, 1984: Wave spectra corrections for measurements with hull-sized accelerometers. *Proc. MTS/IEEE Oceans 1984 Conf.,* Washington, DC, Institute of Electrical and Electronics Engineers, 725–730.

Forristall, G. Z., 2007: Comparing hindcasts with wave measurements from hurricanes Lili, Ivan, Katrina, and Rita. *Proc. 10th Int. Workshop on Wave Hindcasting and Forecasting and Coastal Hazards Symp.,* Oahu, HI, U.S. Army Engineer Research, 20 pp. [Available online at http://www.waveworkshop.org/10thWaves/Papers/Forristall.pdf.]

Howden, S., S. Bisnath, D. Dodd, D. Wells, and D. Wiesenburg, 2004: Long baseline PPK GPS in the marine environment: An ocean buoy. *Proc. Canadian Hydrographic Conf.,* Ottawa, Canada, Canadian Hydrographic Service, CD-ROM.

——, D. Gilhousen, N. Guinasso, J. Walpert, M. Sturgeon, and L. Bender, 2008: Hurricane Katrina winds measured by a buoy-mounted sonic anemometer. *J. Atmos. Oceanic Technol.,* **25,** 607–616.

Institute of Electrical and Electronic Engineers, 1994: IEEE standard for inertial sensor terminology. IEEE Standard 528-1994, 24 pp.

Kinsman, B., 1965: *Wind Waves—Their Generation and Propagation on the Ocean Surface.* Prentice-Hall, 676 pp.

Lang, N., 1987: The empirical determination of a noise function for NDBC buoys with strapped-down accelerometers. *Proc. IEEE Conf. of Oceans '87,* Halifax, NS, Canada, Institute of Electrical and Electronics Engineers, 225–228.

Longuet-Higgins, M. S., 1985: Accelerations in steep gravity waves. *J. Phys. Oceanogr.,* **15,** 1570–1579.

——, 1986: Eulerian and Lagrangian aspects of surface waves. *J. Fluid Mech.,* **173,** 683–707.

National Data Buoy Center, 2003: Nondirectional and directional wave data analysis procedures. NDBC Tech. Doc. 03-01, 37 pp.

——, cited 2008: How are significant wave height, dominant period, and wave steepness calculated? NDBC, Stennis Space Center. [Available online at www.ndbc.noaa.gov/wavecalc.shtml.]

NOAA, cited 2009: A national operational wave observation plan. NOAA Integrated Ocean Observing System. [Available online at http://ioos.gov/library/wave_plan_final_03122009.pdf.]

Steele, K. E., and M. D. Earle, 1979: The status of data produced by NDBO wave data analyzer (WDA) systems. *Proc. MTS/IEEE Oceans 1979 Conf.,* New York, NY, Institute of Electrical and Electronics Engineers, 212–220.

——, E. L. Burdette, and A. Trampus, 1978: A system for routine measurement of directional wave spectra from large discus buoys. *Proc. MTS/IEEE Oceans 1978 Conf.,* Washington, DC, Institute of Electrical and Electronics Engineers, 614–621.

Taagepera, R., 2009: Why we should shift to symmetric regression. *Making Social Sciences More Scientific, Oxford Scholarship Online Monogr.,* Vol. 23, Oxford Scholarship Online, 154–176.

Tucker, M. J., 1956: A shipborne wave recorder. *Trans. Roy. Inst. Nav. Archit.,* **98,** 236–246.

——, 1959: The accuracy of wave measurements made with vertical accelerometers. *Deep-Sea Res.,* **5,** 185–192.